# Kinetics and reactional pathway of Imazapyr photocatalytic degradation Influence of pH and metallic ions

Marion Carrier [a,*], Nathalie Perol [a], Jean-Marie Herrmann [a], Claire Bordes [b],
Satoshi Horikoshi [c], Jean Olivier Paisse [d], Robert Baudot [d], Chantal Guillard [a]

[a] *Laboratoire d'Application de la Chimie à l'Environnement (LACE), Université Claude Bernard Lyon 1,
43 Bd du 11 Novembre 1918, 69100 Villeurbanne, France*
[b] *Laboratoire de Chimiométrie, UMR Sciences Analytiques, 43 Bd du 11 Novembre 1918, 69622 Villeurbanne Cedex, France*
[c] *Department of Chemistry, Mei Sei University, 2-1-1-Hodokubo, Hino, Tokyo 191-0042, Japan*
[d] *Service Central d'Analyse du CNRS, Echangeur de Solaize, B.P. 22, 69390 Vernaison, France*

## Abstract

Some of advanced oxidation processes (AOP) are characterised by a special chemical feature: the ability to use the high reactivity of $^\bullet$OH radicals in driving oxidation processes. These radicals are suitable for achieving the complete abatement, even including the mineralization of less reactive pollutants.

In this study, a photocatalytic process is used to degrade one herbicide of the imidazolinone family, Imazapyr. It was shown to be photodegraded rapidly and extensively in an aqueous solution. The decline of Imazapyr concentration in the solution followed a first-order kinetics. The apparent first order rate constant was found equal to 0.19 min$^{-1}$ in distilled water at natural pH 3.8. The smaller activities found at acidic and basic pH were explained by considering the ionisation state of Imazapyr and the charge density of TiO$_2$.

The present work dealt with the influence of metal ions like Ni$^{2+}$ and Cu$^{2+}$ which are frequently present in agricultural wastewater on the photocatalytic efficiency of TiO$_2$ in the elimination of Imazapyr. A detrimental effect of the presence of metallic species was observed only with samples containing amount of copper and nickel in the presence of TiO$_2$. Several hypotheses were proposed to explain this phenomenon, passivation of TiO$_2$ surface by adsorption of Cu$_2$O and/or Cu$^0$, formation of a complex or recombinaison of the e$^-$/h$^+$ pairs. At higher concentrations of metallic species like Cu$^{2+}$ and Ni$^{2+}$, a plateau was reached which could be explained by the photo-Fenton like reaction.

In an attempt to understand the basic mechanisms of the degradation of Imazapyr in water by TiO$_2$ photocatalysis, we discussed the primary degradation mechanism on the basis of the experimental results together with molecular orbital calculation of frontier electron density and partial charge.

## 1. Introduction

New oxidation methods or "advanced oxidation processes" (AOP) were used in order to degrade organic compounds. Heterogeneous photocatalysis appears as an emerging destructive technology leading to the total mineralization of many organic pollutants.

Photocatalytic process begins when the TiO$_2$ particles absorb light at a wavelength smaller than 384 nm. Consequently, valence band electrons are promoted through the bandgap into the conduction band, generating an electron–hole (e$^-$/h$^+$) pair. These pairs are able to initiate oxidation and reduction reactions at the TiO$_2$ surface. The positive holes can oxidize the organic molecules adsorbed at the surface, through the formation of $^\bullet$OH radicals. On the other hand, the photogenerated electron can produce radical species such as superoxide O$_2^{\bullet-}$ and hydroperoxide HO$_2^{\bullet-}$. All these radicals initially oxidize the substrate in intermediates which subsequently undergo a complete mineralization.

* Corresponding author. Tel.: +33 4 72 44 54 83; fax: +33 4 72 44 53 99.
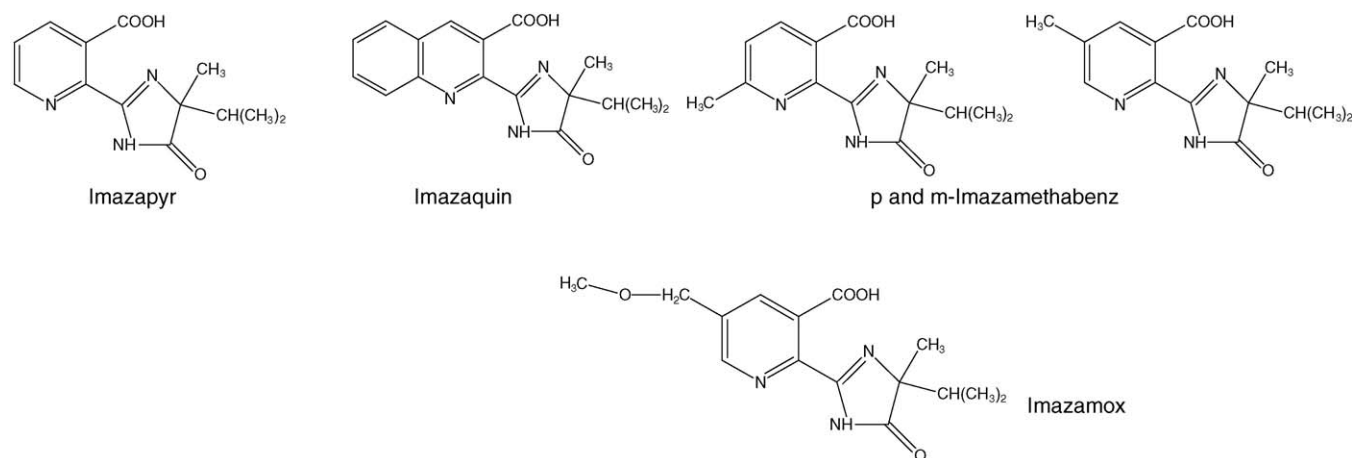*E-mail address:* marion.carrier@catalyse.cnrs.fr (M. Carrier).

Fig. 1. Structural formula of the imidazolinone herbicides.

Many investigations concerning environmental decontaminations had been performed using $TiO_2$ photocatalysis as advanced oxidative processes [1–8].

Agricultural development had caused great damage to the environment. The extensive use of pesticides had polluted soils and waters. We had focused our study on Imidazolinone family which shows different structures (Fig. 1).

This study dealt with Imazapyr which was used for vegetation control in forest and rights of way, rubber plantations and oil palm plantations. Imazapyr was manufactured by American Cyanamid Co. and sold under the trade names Arsenal, Chopper and Assault. It was first registered in the United States in 1984.

Despite of his prohibition in France in July 2002, we could notice its persistence in soil. Imazapyr move readily in soil. It had contamined surface and ground water. Like all members of the imidazolinone family of herbicide, Imazapyr kills plants by inhibiting the first enzyme used when plants synthesize branched chain amino acids (Valine, Leucine and Isoleucine). Within a few hours after treatment with Imazapyr, synthesis of DNA and cell division stops. Complete death of the plant occurs slowly, taking as long as a month after treatment. Moreover Imazapyr is corrosive to both eyes and skin.

In the literatures we could notice several studies on Imidazolinone degradations by photolysis [9–14] and few on photocatalytic degradations [15,16].

In agricultural wastewater, herbicides were observed in the presence of metallic ions after a constant and long usage of chemical fertilizers ($CuSO_4$, ...) and different pesticides. The pollution of water has been increased particularly in France. The Morcille, a Beaujolais river was controlled. River water samples were collected in three seasons per year and analyzed for different physicochemical parameters to assess river quality. Concentrations of heavy metals were found $8\ \mu g\,L^{-1}$ for copper and low concentrations of nickel. Moreover, in waterway copper and nickel were found with a concentration of $0.2\ \mu g\,L^{-1}$ [17]. Because of these found high concentrations, some studies had investigated the influence of dissolved metal ions on photocatalysis [18–24]. Generally, in the presence of metal ions $M^{n+}$ the photogenerated electrons and holes may be involved in the surface reduction and oxidation processes [18]:

$$M^{n+} + e^- \rightarrow M^{(n-1)+}$$

$$M^{(n-1)+} + h^+ \rightarrow M^{n+}$$
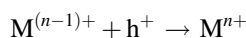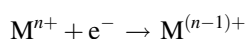
The influence of dissolved metal ions on the photocatalytic degradation rate may be approximately estimated by comparing the standard reduction potential of metal ions to the band edge potentials of $TiO_2$. Positive and/or negative effects occurred along the pollutant degradation. First, various positive effects could be present:

- Lam et al. [19] investigated the effect of charge trapping species of cupric ions on the photocatalytic oxidation of resorcinol. The initial rate of photocatalysis mineralization and degradation of resorcinol was improved by 400%. The beneficial effect of cupric ions was attributed to two phenomena: the formation of a complex between the pollutant and copper which allowed cupric ions to be closer to the catalyst surface and participate in the photoredox cyclic reaction, a scavenging process producing oxidant species.
- During photocatalysis degradation, the $Fe^{2+}$ caused the $Fe^{3+}$ formation, agents allowing photo-Fenton and Fenton reactions. Ghiselli et al. studied the influence of low metallic ion concentrations such as $Fe^{2+}$ [20]. Moreover, some researchers like Okamoto et al. [21], Butler and Davis [22], Bideau et al. [23] and Wei et al. [24] investigated on the catalytic effect of $Cu^{2+}$ ions on the decomposition of $H_2O_2$ to generate $^\bullet OH$ radicals via homogeneous photo-Fenton type like reaction $Cu^{2+} + e^- \rightarrow Cu^+$; $Cu^+ + H_2O_2 \rightarrow Cu^{2+} + OH^- + {}^\bullet OH$.

In other hand, negative effects occured:

- Cu(I)/Cu(II) couple could create a cyclic process without the generation of $^\bullet OH$ radical. This reaction was also known as short circuiting reaction ($Cu^{2+} + e^- \rightarrow Cu^+ + h^+ \rightarrow Cu^{2+}$) and usually occurs at high concentration of $Cu^{2+}$ ion [21,23].

- Brezova et al. confirmed the presence of $Cu_2O$ by IR on the catalyst surface for concentrations higher than 1 mM. Copper deposited on the $TiO_2$ surface may modify the processes of generation and recombination of the charge carriers and intermediates [18].
- Another negative effect could be due to the intensification of light filtering effect by the high concentrations of $Cu^{2+}$ ions which reduces the amount of light available for catalyst activation.

In this paper, we reported the results of the photocatalytic degradation of Imazapyr by $TiO_2$ powder. The influence of the irradiation intensity and of the amount of copper often used in vineyards had been studied. We had discussed the role of pH and copper during Imazapyr degradation. Finally, we had studied the primary intermediate products formed and established degradation pathways of Imazapyr.

## 2. Experimental

### 2.1. Materials

The most popular commercial $TiO_2$ is P-25 produced by the German Company Degussa. $TiO_2$ exists under two main crystallographic forms, anatase and rutile. Anatase has always been found to be photocatalytically more active than rutile [25,26]. $TiO_2$ used in our study was $TiO_2$ Degussa P-25. This sample contains ca. 80% anatase and 20% rutile. Its BET surface area is ca. $50 \ m^2 \ g^{-1}$. Imazapyr herbicide and $Cu(NO_3)_2$ and $Ni(NO_3)_2$ were purchased from Aldrich. In order to adjust the initial pH, $HNO_3$ and NaOH solutions were obtained from Aldrich.

### 2.2. Photoreactor and light source

The batch photoreactor was a cylindrical flask made of Pyrex of ca. 100 mL with a bottom optical window of ca. 4 cm diameter which was open to the air. UV irradiation was provided by a high pressure mercury lamp and was filtered by a circulating-water cell equipped with a 340 nm cut-off filter (Corning 0-52). The water cell was used to remove IR radiation, thus preventing any heating of the suspension.

The radiant flux was measured with a radiometer detector model VLX 3W Bioblock scientific. The response bandwidth of the radiometer was centered on 365 nm. The result gave approximately $6 \ mW \ cm^{-2}$ at this wavelength, corresponding to a total of UV equal to $14.1 \ mW \ cm^{-2}$.

### 2.3. Photodegradation

The photocatalytic test was performed at room temperature (20 °C), 50 mg $TiO_2$ were added, under stirring, to 20 mL of a 20 ppm (80 $\mu mol \ L^{-1}$) solution of the pesticide and maintained in the dark for 30 min to reach the adsorption equilibrium. At time $t = 0$, the photoreactor was irradiated. Samples from the suspension (0.5 mL) were taken at regular time intervals for analysis. The amount of 50 mg of titania was chosen, since, in

our conditions, there is a complete adsorption of the UV-light entering the photoreactor.

### 2.4. Analytical determination

Samples taken after different times of irradiation, were filtered through 0.45 $\mu m$ filters (Millipore) to remove $TiO_2$ particles before analysis.

The HPLC-UV analyses were performed using a VARIAN system with a diode array and on a 125 mm × 4 mm C18 reverse-phase column (Hypersil BDS). The mobile phase composition was methanol and a phosphoric acid aqueous buffer adjusted to pH 2.8 at a ratio 20:80.

The eluant flow rate was fixed (1 mL $min^{-1}$). The detection wavelength was set at 254 nm.

The complexation was studied with UV spectrometer and copper concentrations were verified by atomic absorption.

Identification of degradation intermediates was determined using LC/MS (electrospray ionisation) in positive mode with (20:80) (methanol; acidified water by formic acid) mobile phase equipped with the C18 reverse-phase column. In order to ameliorate results in LC–MS, we made a preconcentration of sample on OASIS hydrophilic balanced copolymer (HLB) cartridge. This manipulation consisted of reducing sample volume of 20 mL in a volume of 500 $\mu L$. Intermediates stocked in the solid phase of cartridge were extracted by 500 $\mu L$ of methanol.

Computer simulations with MOPAC allowed to calculate the frontier electron density used to assess the positions of •OH radical attack and the partial charge in Imazapyr.

## 3. Results and discussions

### 3.1. Kinetics of Imazapyr degradation

It was experimentally verified that direct photolysis of the substrate was very slow under UV irradiation alone (Fig. 2). Furthermore, under our conditions the concentration in Imazapyr was ever observed when the adsorption was carried out in the dark for the catalyst used.

Imazapyr was shown to photodegrade rapidly and extensively. In 20 min, we could observe the total disappearance of Imazapyr. Moreover, the total organic carbon (TOC) had been followed and showed the efficiency of photocatalysis to mineralize an organic compound. More than 92% of TOC had totally disappeared in about 24 h (Fig. 2b). Imazapyr concentration abatement in the solution followed first-order kinetics. The apparent first order rate constant $k$ was found equal to 0.19 $min^{-1}$ in distilled water at natural pH 3.8 for $TiO_2$ powder (Figs. 2–4).

### 3.2. Effect of the radiant flux of the irradiation source

In literature [4], the rate was found to be proportional to the radiant flux $\Phi$ for $\Phi < 25 \ mW \ cm^{-2}$. Above 25 $mW \ cm^{-2}$, $r$ varied as $\Phi^{1/2}$, indicating a too high value of the flux and an increase of the electron–hole recombina-
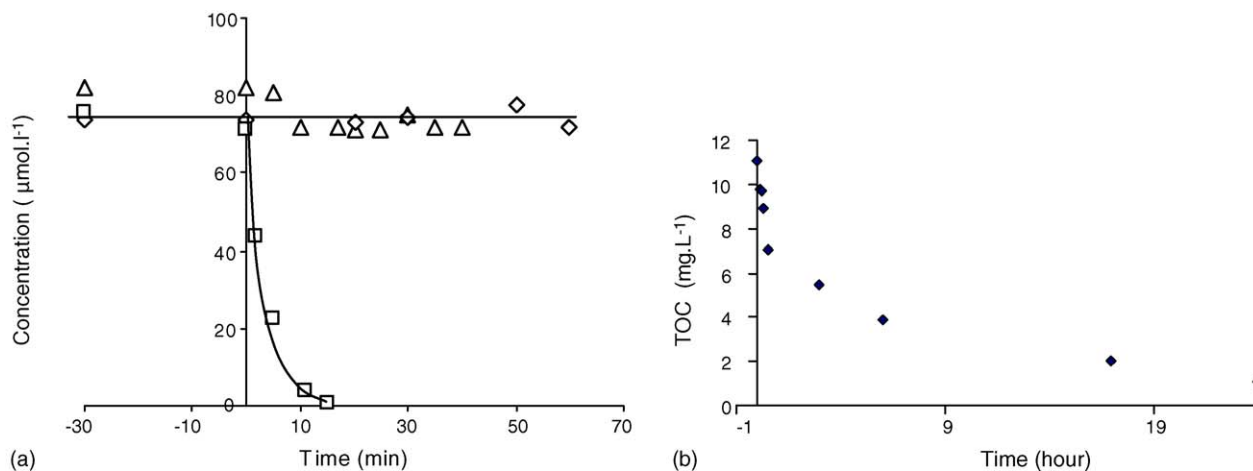
Fig. 2. (a) ($\diamond$) Photolytic degradation, ($\square$) photocatalytic degradation of Imazapyr, ($\triangle$) adsorption in the dark with TiO$_2$ powder. (b) Kinetics of TOC Imazapyr disappearance.
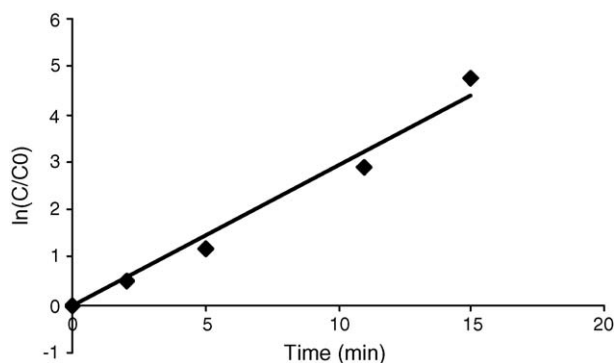


Fig. 3. First-order linear transforms ln ($C_0/C$) = $f(t)$. Conditions: $C_0 = 75.8$ $\mu$mol L$^{-1}$, m(TiO$_2$) = 2.5 g L$^{-1}$, $V$ = 20 mL, $T$ = 20 °C, natural pH values.

tion rate. The rate constant of disappearance of Imazapyr (initial concentration of 80 $\mu$mol L$^{-1}$) under different intensity radiations was shown in Fig. 4. In our experimental conditions rate constants were found to be directly proportional to the radiant flux which was the optimal light power utilization at natural pH 3.8 and confirmed the theory.

### 3.3. Effect of pH

In this study, the initial pH was adjusted at 2.1 by addition of HNO$_3$, 3.8 (pH natural), 6.4, 7.1 and 8.4 by addition of NaOH in an aqueous solution of Imazapyr (80 $\mu$mol L$^{-1}$) with TiO$_2$ powder (2.5 g L$^{-1}$). Guillard et al. [27] showed that sodium and nitrate had a low impact on the degradation of methylene blue at neutral and basic pH. The introduction of new ions such as Na$^+$ and NO$_3^-$ had a low influence on the rate constant in comparison with pH.

Fig. 5 showed that degradation occurred more rapidly at pH 3.8. This behaviour depended on the type of interactions between Imazapyr molecules and the catalyst surface. Therefore Imazapyr exhibits five distinct chemical species that are presented in Fig. 6. The acid–base dissociation constants of the various functional groups had been determined to be 1.88, 3.6 and 10.8 [9].

On the other hand, the PZC of TiO$_2$ is equal to 6.3. This means that the TiO$_2$ surface is positively charged (Ti–OH$_2^+$) when the pH is lower than this value and negatively charged (Ti–O$^-$) when the pH is higher than PZC. Interactions are going to accelerate or retard the degradation.

Table 1 shows form distribution in function of pH obtained by following calculations:

$$c = [III] + [II] + [IV]$$

$$K_{a_1} = 10^{-1.88} = [III] \times [H_3O^+]/[II]$$



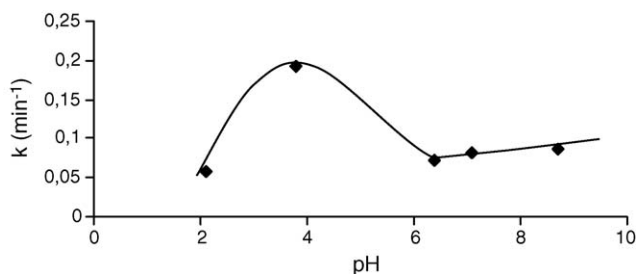Fig. 4. Influence of the radiation intensity on the rate constant.
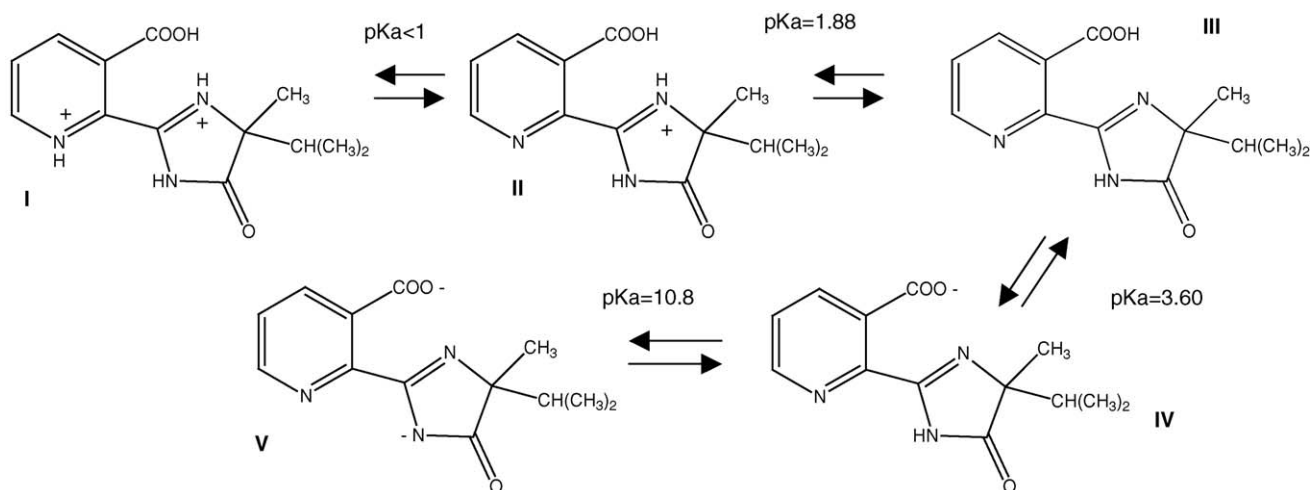


Fig. 5. Rate constant (min$^{-1}$) at different pH values.

Fig. 6. Different forms of Imazapyr as a function of the pH.

$$K_{a_2} = 10^{-3.6} = [IV] \times [H_3O^+]/[III]$$

$$K_{a_2} \times K_{a_1} = [IV] \times [H_3O^+]^2/[II]$$

$$K_{a_2} \times K_{a_1} = [H_3O^+]^2/[II] \times (c - [III] + [II])^2$$

$$[III] = K_{a_1} \times [II]/[H_3O^+]$$

$$K_{a_2} \times K_{a_1} = [H_3O^+]^2/[II] \times (c - K_{a_1} \times [II]/[H_3O^+] + [II])^2$$

$$K_{a_2} \times K_{a_1}/[H_3O^+]^2 = c/[II] - K_{a_1}/[H_3O^+] - 1$$

$$[II] = c/K_{a_2} \times K_{a_1}/[H_3O^+]^2 + K_{a_1}/[H_3O^+] + 1$$

$$[III] = K_{a_1} \times [II]/[H_3O^+]$$

$$[IV] = K_{a_2} \times [III]/[H_3O^+]$$

with $K_{a_1}$ and $K_{a2}$ acid constants and [II], [III], [IV] Imazapyr form of concentrations.

In this present study, the degradation rate increases with the increase in pH from 2.1 to 3.8 and decreases with the pH from 3.8 to 8.4.

At pH 2.1, neutral species III were dominant (60%) and TiO$_2$ surface was charged positively, interactions were low. At pH natural 3.8, the carboxylate ion specie IV was dominant (61%) and may theoretically existed with neutral species III (38.5%). Interactions between TiOH$_2^+$ and

Imazapyr were very strong and allowed Imazapyr to be degradated more easily. On the other hand, at pH > 6.3 (PZC) TiOH and TiO$^-$ species were present. Imazapyr and TiO$_2$ surface existed under negative forms. Therefore, repulsions were much more marked because both species were negatively charged, thus preventing interactions and delaying degradation. Optimal domain for Imazapyr degradation was pH 3.8.

The type of interactions between organic forms and catalyst surface was very important in the pollutant degradation.

### 3.4. Effect of copper and nickel amount

The disappearance rate of Imazapyr decreases as a function of copper and nickel ion concentration before reaching a pseudo-plateau (Figs. 7 and 8).

Whatever the concentration of copper and nickel ions, the rate constant decreased. When the plateau was reached the efficiency was decreased with a factor of 4 for the Copper and with a factor of 2 for the nickel (Figs. 9 and 10). Behaviours of Cu$^{2+}$ and Ni$^{2+}$ were complex.

Table 1
Effect of pH on the degradation rate constant and of the presence of species in percent

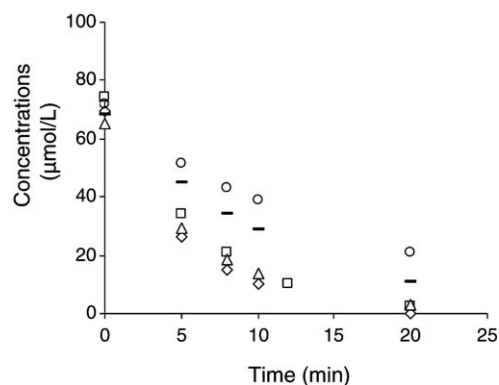| pH | $k$ (min$^{-1}$) | Specie III % neutral form | Specie IV % negative form | Specie II % positive form | Major forms of TiO$_2$ |
|---|---|---|---|---|---|
| 2.1 | 0.06 | 60 | 4 | 36 | TiOH, TiOH$_2^+$ |
| 3.8 | 0.19 | 38.5 | 61 | 0.5 | TiOH, TiOH$_2^+$ |
| 6.4 | 0.07 | 0.3 | 99.7 | 0 | TiOH |
| 7.1 | 0.08 | 0.1 | 99.9 | 0 | TiO$^-$ |
| 8.4 | 0.09 | 0 | 100 | 0 | TiO$^-$ |



Fig. 7. Photocatalytic degradation of Imazapyr in the presence of Cu$^{2+}$: (◇) without Cu$^{2+}$, (□) with 0.04 mmol L$^{-1}$, (△) with 0.06 mmol L$^{-1}$, (▬) with 0.16 mmol L$^{-1}$, (○) with 0.31 mmol L$^{-1}$.
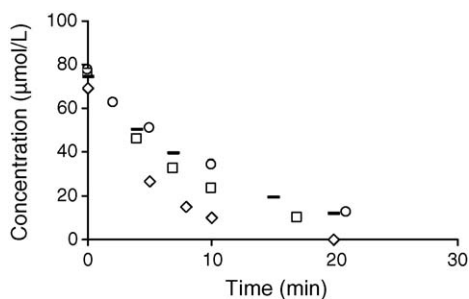
Fig. 8. Photocatalytic degradation of Imazapyr in the presence of $Ni^{2+}$: ($\diamondsuit$) without $Ni^{2+}$, ($\square$) with 0.04 mmol $L^{-1}$, ($\triangle$) with 0.06 mmol $L^{-1}$, ($\blacksquare$) with 0.16 mmol $L^{-1}$, ($\circ$) with 0.31 mmol $L^{-1}$.
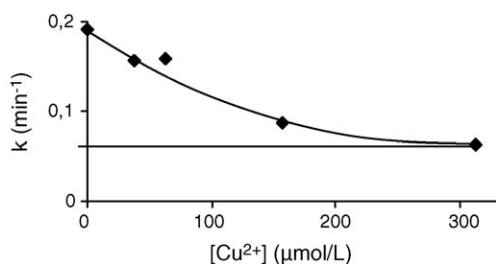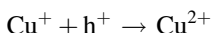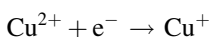


Fig. 9. Kinetic constants for different $[Cu^{2+}]$.

First, the detrimental effect could be induced by a competitive trapping of oxidizing species following these equations:

$$Cu^{2+} + e^- \rightarrow Cu^+$$

$$Cu^+ + h^+ \rightarrow Cu^{2+}$$

The reduction of $Cu^{2+}$ by photogenerated electrons followed by the oxidation of $Cu^+$ may be in competition with the formation of superoxide anion radicals and hydroxyl radicals and consequently may reduce the disapperance rate of Imazapyr molecules.

Moreover the photodeposition of copper species such as $Cu^0$ and $Cu_2O$ at $TiO_2$ surface could be present. The determination of $E$–pH diagram showed each domain in which one species was the most thermodynamically stable. $Cu^0$ and $Cu_2O$ could coexiste [28].

These copper oxides had been detected by Yamazaki et al. using IR analysis [29]. This may modify the process of
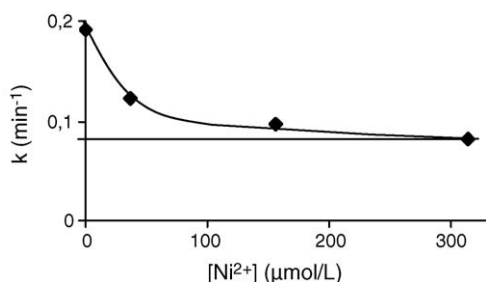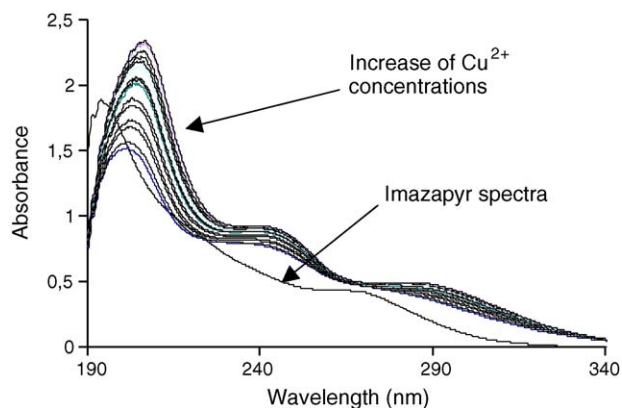


Fig. 10. Kinetic constants for different $[Ni^{2+}]$.



Fig. 11. UV spectra of Imazapyr–$Cu^{2+}$ complex as a function of molar ratio between Imazapyr (constant concentration of 75 $\mu$mol $L^{-1}$) and $Cu^{2+}$ (variable concentration between 19 and 56 $\mu$mol $L^{-1}$).

generation and recombination of the charge carriers and radical intermediates.

Finally, Quivet et al. reported the formation of neutral complex structures of $Cu^{2+}$ ions with Imazapyr in the suspensions. In our experimental conditions, the complex formed by herbicide Imazapyr with $Cu^{2+}$ was identified by UV spectrometry with the molar ratio technique [30,31].

The formation of a complex Imazapyr-$Cu^{2+}$ in our experimental conditions was confirmed by UV measurement (Fig. 11). At 267 nm, an isobestic point was present. It allowed
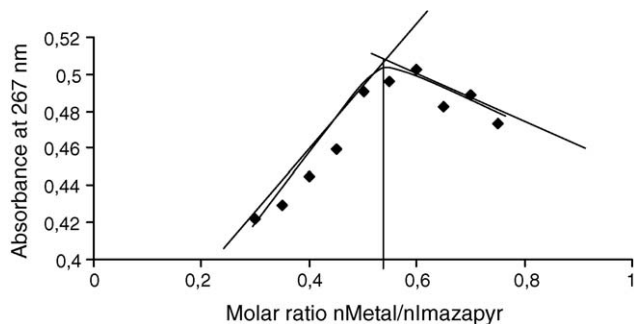


Fig. 12. Representation of absorbance as function of ratio molar metal on Imazapyr.
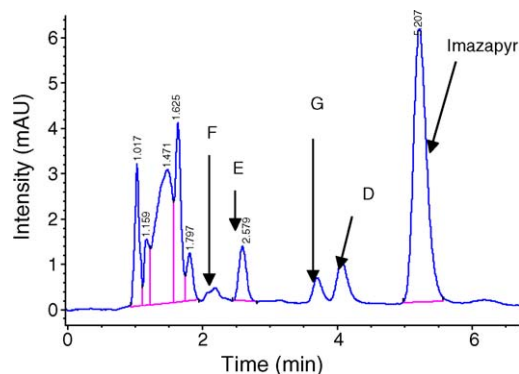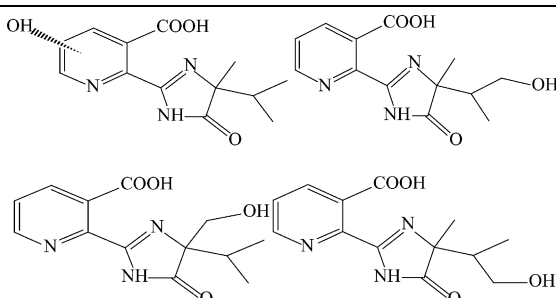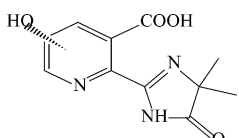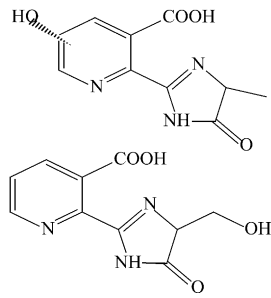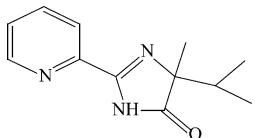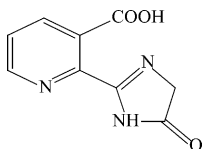


Fig. 13. LC–MS chromatogram of Imazapyr degradation by photocatalysis after 10 min.
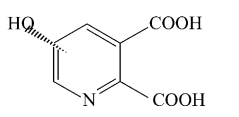
to represent the absorbance at 267 nm as a function of the molar ratio curve (Fig. 12).

The result allowed to confirm that the complex was constituted by two molecules of Imazapyr and one molecule of $Cu^{2+}$ ions: $[Cu(Imz)_2 \cdot 2H_2O]$ [30–32]. This particular behaviour (complex formation) with metallic salts [30,32–34] could be reduced or enhanced Imazapyr degradation by photochemistry [35].

Table 2
Structure of photoproducts of the Imazapyr degradation identified by LC/MS electrospray in positive and negative modes

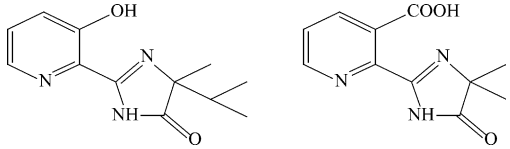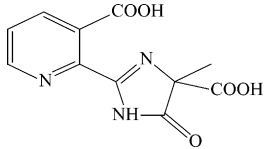| | Structure | Retention time ES+ (min) | ES positive M + H | ES negative M − H | M |
|---|---|---|---|---|---|
| $D_1, D_2, D_3, D_4$ |  | 7.888, 4.310, 4.107, 2.236 | 278 | 276 | 277 |
| E |  | 2.605, 1.662, 1.390 | 250 | 248 | 249 |
| G |  | 3.722 | 184 | 182 | 183 |
| F |  | 2.154, 1.092 | 236 | 234 | 235 |
| C |  | 4.078, 1.641 | 234 | 232 | 233 |
| H |  | 5.2 | 264 | 262 | 263 |
| A |  | 5.2 | 218 | | 217 |
| I |  | | | 204 | 205 |

At higher $Cu^{2+}$ concentrations, these detrimental effects were reduced. This behaviour could be due to the formation of $^{\bullet}OH$ by photo-Fenton in the presence of $H_2O_2$ formed on $TiO_2$ [22,36,37]:

$$M^{(n-1)+} + H_2O_2 \rightarrow M^{n+} + {}^{\bullet}OH + OH^-$$
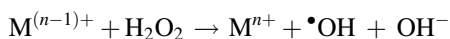
Fenton's reagent is composed of a solution containing hydrogen peroxide and a $Fe^{2+}$ salt, in an acidic medium. Ferric and $Cu^{2+}$ ions (Fenton-like reagents) could be also used in Fenton-like reaction. The efficiency of the Fenton reagent for destruction of organic matter can be enhanced by irradiation with light in the UV range (photo-Fenton reaction) [20,38]. After degradation of twenty different dyes in aqueous solutions by the Fenton process, Xu et al. found catalytic activity of metal ions was measured to be in the following sequence: $Fe^{2+} > Cu^{2+} > Mn^{2+} > Ag^+$. Under UV irradiation, the same sequence of the catalytic activity of the metal ion was obtained with an improvement by UV irradiation assistance [38].

## 3.5. Identification of intermediate products by electrospray mass spectroscopy

After 10 min of irradiation, we had stopped the reaction and preconcentred on a cartridge in order to improve results. The following chromatogram (Fig. 13) corresponds to a photo-catalytic degradation of Imazapyr under an irradiation of 6 mW cm$^{-2}$ at 365 nm.

Structures of products identified in LC/MS were present in Table 2. Some peaks appeared at 183, 205, 217, 233, 235, 249, 263 and 277 $m/z$ which could be assigned to the chemical structures, G, I, A, C, F, E, H and $D_{1-4}$ (Scheme 1). These were attributed to: (i) the hydroxylation of aromatic ring or methyl group, $D_{1-4}$ (Scheme 1), (ii) to the successively oxidation of aliphatic chain of E, F and I (Scheme 1) (loss of two methyl groups) and (iii) opening of imidazoline cycle and bonding rupture between the two cycles (compound G, Scheme 1).

At this irradiation time first intermediates began to disappear. After extraction of different mass detected by
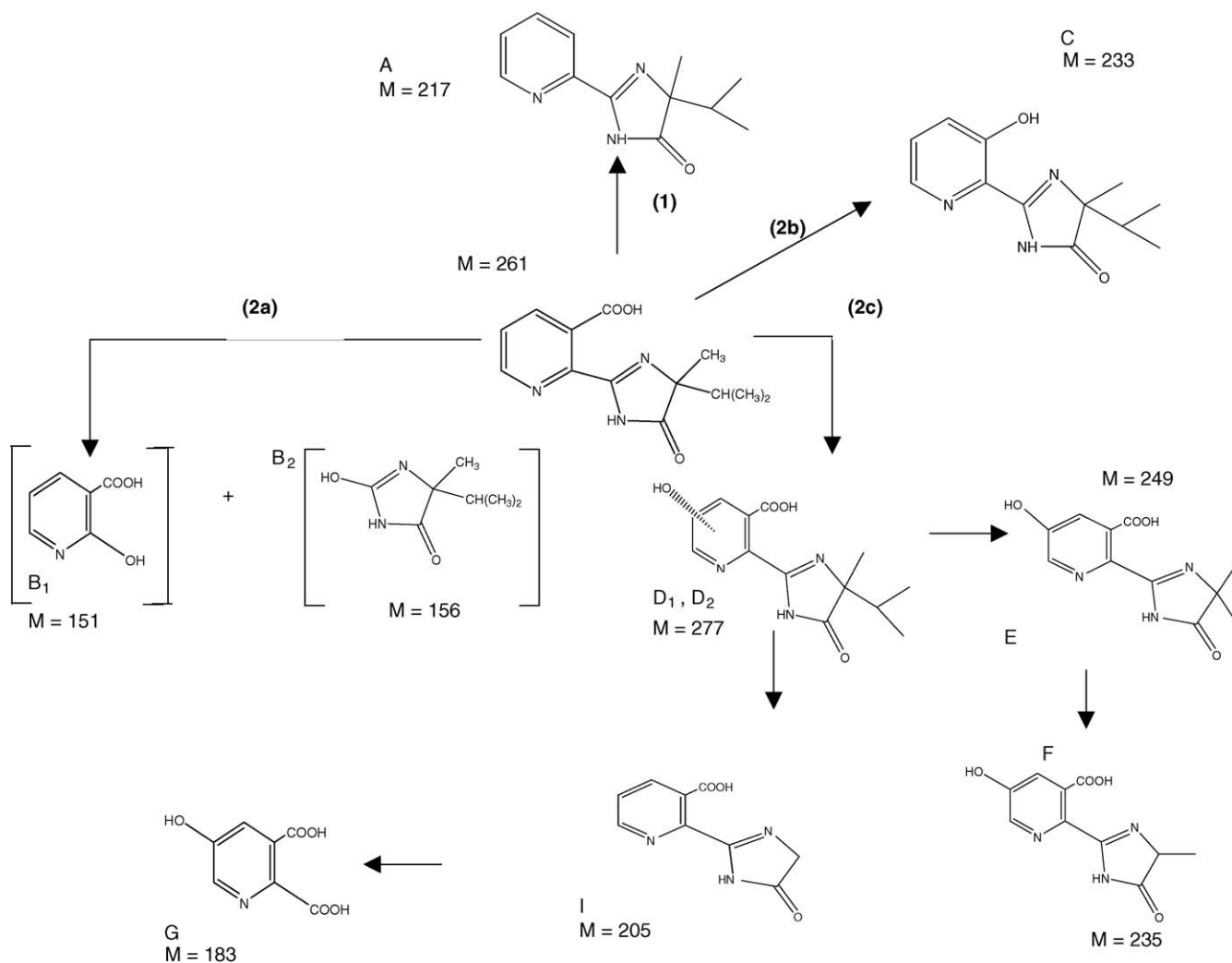


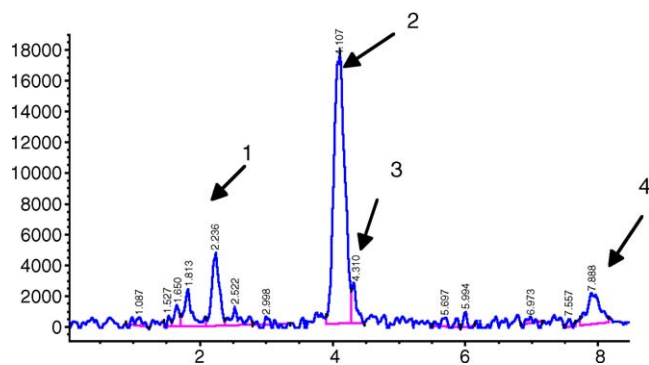Scheme 1. Degradation pathways of Imazapyr.

Fig. 14. Mass spectra of the extraction 278 *m/z* in positive electrospray mode corresponding to $D_{1-4}$ products.



Fig. 15. Chemical structure with the atom numbers used in the molecular orbital calculation.

LC–MS, some isomers and new structures were found and were presented in Table 2 (Fig. 14).

Four isomers of hydroxylated products with a mass of 218 were present at different retention times.

### 3.6. Photocatalytic mechanism

Frontier electron densities and point charges of all individual atoms in the Imazapyr were calculated using the CAChe system in the MOPAC program; the resulting values are summarised in Table 3 (Fig. 15):

The adsorption position was important in the decomposition of organic substance. Indeed, the life time of $^\bullet OH$ and $^\bullet OOH$ radicals was very short and the degradation was caused on the $TiO_2$ surface. The calculation of point of charge shown different points of adsorption and the calculation of electronic density shown attack position of $^\bullet OH$ and $^\bullet OOH$ radicals.

#### 3.6.1. Interpretation of point charge calculation [39,40]

For Imazapyr the most negative point charges were located on the oxygen atoms $O^1$ and $O^3$. We expected therefore that the point of adsorption of the Imazapyr at pH natural be through the carboxylic group. We could not preclude partial adsorption of Imazapyr through its nitrogen atom $N^{13}$.

#### 3.6.2. Interpretation of electronic density calculation [39,40]

In photocatalysis two species were important holes $h^+$ and hydroxyl radicals $^\bullet OH$.

Holes could directly oxidize Imazapyr according to a ''Photo-Kolbe'' reaction with decarboxylation of pyridinic cycle proved by the presence of A compound 217 *m/z* (Pathway 1, Scheme 1). This confirmed that the preferential mode of adsorption of Imazapyr was related to the binding of the carboxylic group at the surface of Titania.

To understand different degradation pathways (2a–2b–2c), the calculation of electronic density was interesting. The primary position for $^\bullet OH$ radical (an electrophilic species) should attack on the atoms with the largest electron density.

For Imazapyr these atoms were the pyridinic $C^5$, $C^7$, $C^8$, $C^{10}$ carbons and $N^{12}$ atom. Primary $^\bullet OH$ radical attack on $C^8$ should lead to the bonding rupture between the two cycles (Pathway 2a, Scheme 1). Products $B_1$ and $B_2$ were not detected under our experimental conditions. This absence of detection could be due to the steric of carboxylic and methyl groups which prevent $^\bullet OH$ radical to attack easily $C^8$ and $C^{11}$ carbons.

A new attack was possible in $C^5$ allowing the formation of C compound 233 *m/z* after a decarboxylation following to an hydroxylation (Pathway 2b, Scheme 1)

Some attacks appeared simultaneously in $C^7$ and $C^{10}$ carbons to form $D_1$ and $D_2$ isomers (Pathway 2c, Scheme 1) confirmed by LC/MS in positive mode.

Methyl group of $D_1$ and $D_2$ compounds were gradually oxidized in alcohol, aldehyde and acid. According to the photo-Kolbe reaction, the decarboxylation and the hydroxylation allowing E and F formations (Pathway 2c, Scheme 1) were expected.

Table 3
Calculated partial charge and radical frontier density for Imazapyr using the MOPAC method

| Atom | Partial charge | Radical frontier density | Atom | Partial charge | Radical frontier density |
|---|---|---|---|---|---|
| $O^1$ | −0.44940 | 0.04154 | $C^{18}$ | −0.22820 | 0.00820 |
| $O^2$ | −0.33660 | 0.01264 | $C^{19}$ | −0.21140 | 0.00854 |
| $O^3$ | −0.43990 | 0.08804 | $H^{20}$ | 0.30490 | 0.00092 |
| $C^4$ | 0.42150 | 0.05194 | $H^{21}$ | 0.19200 | 0.00088 |
| $C^5$ | −0.14060 | 0.26215* | $H^{22}$ | 0.19410 | 0.00044 |
| $C^6$ | −0.02560 | 0.09273 | $H^{23}$ | 0.21110 | 0.00071 |
| $C^7$ | −0.16900 | 0.22961* | $H^{24}$ | 0.31260 | 0.00169 |
| $C^8$ | 0.07370 | 0.29617* | $H^{25}$ | 0.10830 | 0.00242 |
| $N^9$ | −0.21100 | 0.06194 | $H^{26}$ | 0.10570 | 0.00257 |
| $C^{10}$ | −0.01620 | 0.22251* | $H^{27}$ | 0.09860 | 0.00145 |
| $C^{11}$ | 0.14280 | 0.08524 | $H^{28}$ | 0.10290 | 0.00744 |
| $N^{12}$ | −0.24710 | 0.22901* | $H^{29}$ | 0.08720 | 0.00202 |
| $N^{13}$ | −0.33850 | 0.16998 | $H^{30}$ | 0.08610 | 0.00218 |
| $C^{14}$ | 0.32550 | 0.03047 | $H^{31}$ | 0.08920 | 0.00386 |
| $C^{15}$ | −0.00180 | 0.02874 | $H^{32}$ | 0.08260 | 0.00298 |
| $C^{16}$ | −0.21190 | 0.01749 | $H^{33}$ | 0.08370 | 0.00129 |
| $C^{17}$ | −0.08000 | 0.03019 | $H^{34}$ | 0.08490 | 0.00202 |

* Atoms with the largest electron density.

Intermediates resulting from the imidazolinic cycle opening of $D_1$, $D_2$ compounds were not detected but the identification of G compound confirms the imidazolinic cycle opening. I compound identified in negative mode by electrospray would completed the 2c pathway allowing to the G product formation.

## 4. Conclusion

Imazapyr was totally degraded in the presence of $TiO_2$ powder after 30 min of adsorption in the dark and 20 min of irradiation following apparent first-order kinetics. The addition of copper (0.4 mol $L^{-1}$ to 0.6 mmol $L^{-1}$) to suspension had no effect on the rate constant but, at higher concentrations, a decrease was observed. The most favorable pH for this degradation was found equal to pH 3.8.

The effect of dissolved metal ions on the photocatalytic degradation rate with $TiO_2$ powder was investigated. The obtained results may be summarised as follows: For low concentrations of $Cu^{2+}$ and $Ni^{2+}$ rate constants decreased. At higher concentrations, a plateau was reached. Negative effects like the photodeposition of $Cu^0$ and $Cu_2O$ and the recombination of $h^+/e^-$ were reduced by the photo-Fenton like reaction at higher concentrations.

This work showed the role of frontier orbital density and adsorption on the degradation pathways.

Three major pathways had been determined in the degradation of Imazapyr by using LC/MS.

These results clearly confirmed that photocatalysis is a convenient and cheap means of decontaminating used waters produced in vinyards.

Independently of vinery activities and because of the robust character of titania, photocatalysis can also be envisaged as an advantageous technique for purifying aqueous wastes and producing drinking water, especially in sunny arid areas for isolated populations [41], where water supply is becoming a crucial problem in the present millennium.

## References

[1] C. Guillard, S. Horikoshi, N. Watanabe, H. Hidaka, P. Pichat, J. Photochem. Photobiol. A: Chem. 149 (2002) 155.

[2] J.-M. Herrmann, C. Guillard, C.R. Acad. Sci. Paris, Série IIc, Chimie/Chemistry 3 (23) 417.

[3] C. Guillard, J. Photochem. Photobiol. A: Chem. 135 (2000) 65.

[4] J.-M. Herrmann, Catal. Today 53 (1999) 115.

[5] D. Robert, S. Malato, Sci. Total Environ. 291 (2002) 85.

[6] M.-J. Farré, M.-I. Franch, S. Malato, J.A. Ayllon, J. Peral, X. Domenech, Chemosphere 58 (2005) 1127.

[7] V. Maurino, C. Minero, E. Pelizzetti, M. Vincenti, Colloids Surf. A: Physicochem. Eng. Aspects 151 (1999) 329.

[8] S. Malato, J. Blanco, J. Caceres, A.R. Fernandez-Alba, A. Agüera, A. Rodriguez, Catal. Today 76 (2002) 209.

[9] N. Moorthy Mallipudi, S.J. Stout, A. daCunha, A.-H. Lee, J. Agric. Food Chem. 39 (1991) 412.

[10] M. El Azzouzi, H. Mountacer, M. Mansour, Fresenius Environ. Bull. 8 (1999) 709.

[11] H.D. Burrows, L. M. Canle, LJ.A. Santaballa, S. Steenken, J. Photochem. Photobiol. B: Biol. 67 (2002) 71.

[12] W.S. Curran, M.M. Loux, R.A. Liebl, F.W. Simmons, Weed Sci. 40 (1992) 143.

[13] G. Mangels, Behaviour of the imidazolinone herbicides in the aquatic environment, in: D.L. Shaner, S.L. O'Connor (Eds.), The Imidazolinone Herbicides, CRC Press, Boca Raton, FL, 1991, , 290 pp. (Chapter 16).

[14] M. Mekkaoui, M. El Azzouzi, A. Bouhaouss, M. Ferhat, A. Dahchour, S. Guittonneau, Meallier, Fresenius Environ. Bull. 9 (2000) 783.

[15] J.C. Garcia, K. Takashima, J. Photochem. Photobiol. A: Chem. 155 (2003) 215.

[16] P. Pizarro, C. Guillard, N. Perol, J.M. Herrmann, Catal. Today 101 (2005) 211.

[17] C.Bliefert, R. Perraud, Chimie de l'Environnement Air, Eau, Sols, Déchets, Deboeck Université Eds, 2001, p. 291.

[18] V. Brezova, A. Blazkova, E. Borosova, M. Ceppan, R. Fiala, J. Mol. Catal. A: Chem. 98 (1995) 109.

[19] S.W. Lam, K. Chiang, T.M. Lim, R. Amal, G.K.-C. Low, Appl. Catal. B: Environ. 55 (2005) 123.

[20] G. Ghiselli, W.F. Jardim, M.I. Litter, H.D. Mansilla, J. Photochem. Photobiol. A: Chem. 167 (2004) 59.

[21] K.I. Okamoto, Y. Yamamoto, H. Tanaka, M. Tanaka, A. Itaya, Bull. Chem. Soc. Jpn. 58 (1985) 2018.

[22] E.C. Butler, A.P. Davis, J. Photochem. Photobiol. A 70 (1993) 273.

[23] M. Bideau, B. Claudel, L. Faurel, M. Rachimoellah, Chem. Eng. Commun. 93 (1990) 167.

[24] T.Y. Wei, Y.Y. Wang, C.C. Wan, J. Photochem. Photobiol. A 55 (1990) 115.

[25] A.H. Boonstra, et al. J. Mol. Catal. A: Chem. 79 (1975).

[26] Y. Ku, R. Leu, K-C. Lee, Water Res. 30 (1996) 2569.

[27] C. Guillard, H. Lachheb, A. Houas, M. Ksibi, E. Elaloui, J.M. Herrmann, J. Photochem. Photobiol. A: Chem. 158 (2003) 27–36.

[28] G. Charlot, Les réactions chimiques en solution, Masson et Cie, Paris, 1969.

[29] S. Yamazaki, et al. J. Photobiol. A: Chem. 161 (2003) 57.

[30] E. Quivet, R. Faure, J. Georges, J. Chem. Crystallogr. 34 (2004) 25.

[31] L.S. Erre, E. Garribba, G. Micera, N. Sardone, Inorg. Chim. Acta 272 (1998) 68.

[32] L. Strinna Erre, E. Garribba, G. Micera, A. Pusino, D. Sanna, Inorg. Chim. Acta 255 (1997) 215.

[33] L. Strinna Ere, E. Garribba, G. Micera, N. Sardone, Inorg. Chim. Acta 272 (1998) 68.

[34] A.M. Duda, M. Dyba, H. Kozlowski, G. Micera, A. Pusino, J. Agric. Food Chem. 44 (1996) 3698.

[35] K.V. Subba Rao, B. Lavédrine, P. Boule, J. Photochem. Photobiol. A: Chem. 154 (2003) 189.

[36] D.L. Sedlak, J. Hoigné, Atmos. Environ. 27A (1993) 2173.

[37] M.I. Litter, Appl. Catal. B: Environ. 23 (1999) 89.

[38] X.-R. Xu, H.-B. Li, W.-H. Wang, J.-D. Gu, Chemosphere 57 (2004) 595.

[39] S. Horikoshi, N. Serpone, J. Zhao, H. Hidaka, J. Photochem. Photobiol. A: Chem. 118 (1998) 123.

[40] S. Horikoshi, N. Watanabe, M. Mukae, H. Hidaka, N. Serpone, New J. Chem. 25 (2001) 999.

[41] C.Guillard, J.M.Herrmann, "AQUACAT" and "SOLWATER" European Programmes (with 12 laboratories and industries for each one).